Journal of Applied Polymer Science

Studies of polylactide/zinc oxide nanocomposites: influence of surface treatment on zinc oxide antibacterial activities in textile nanocomposites

Awa Soronfé Doumbia,[1,2] Hervé Vezin,[3] Manuela Ferreira,[1,2] Christine Campagne,[1,2] Eric Devaux[1,2]

[1]University Lille Nord de France, Lille F-59000, France

[2]Ecole Nationale Superieure des Arts et Industries textiles (ENSAIT), GEnie et Materiaux Textiles (GEMTEX), Roubaix F-59100, France

[3]LAboratoire de Spectrochimie Infrarouge et Raman (LASIR) Centre National de la recherche scientifique (CNRS), Villeneuve d'Ascq F-59650, France

Correspondence to: A. S. Doumbia (E-mail: awasoronfe@gmail.com)

ABSTRACT: Polylactide (PLA)/zinc oxide (ZnO) nanocomposite filaments were produced with a melt-spinning process, with the aim of obtaining antibacterial textiles. ZnO, an inorganic antibacterial nanofiller, is used to impart antibacterial properties to PLA. These nanoparticles suit the melt-spinning process because of their high thermal stability and low granulometry. Generally, metallic oxides (e.g., ZnO) are used to recycle PLA via catalyzed unzipping depolymerization. In this study, we used different ways to finely disperse ZnO in PLA and produce filaments with a minimum degradation of the thermal and mechanical properties. Optimized antibacterial properties were obtained with a fabric containing ZnO with specific surface treatments. The reasons for this better antibacterial activity, related to the study of the antibacterial mechanism of ZnO, were investigated with different characterization techniques [X-ray, electron probe microanalysis, inductively coupled plasma mass spectrometry, and electron paramagnetic resonance (EPR)]. © 2015 Wiley Periodicals, Inc. J. Appl. Polym. Sci. **2015**, *132*, 41776.

KEYWORDS: biodegradable; biomedical applications; biopolymers and renewable polymers; fibers; nanostructured polymers

Received 28 April 2014; accepted 5 November 2014

DOI: 10.1002/app.41776

INTRODUCTION

Nanoparticles generally exhibit better physicochemical properties than microparticles,[1] thanks to their higher surface-to-volume ratio. Zinc oxide (ZnO) nanoparticles are interesting materials because of their multifunctional properties and low cost. ZnO is an *n*-type semiconductor with a wide direct band gap of 3.37 eV and a high exciton binding energy of approximately 60 meV.[2] These characteristics provide them with several properties, mainly photocatalytic and antibacterial properties.[3] In this study, we focused particularly on the antibacterial properties brought about by the addition of ZnO in a spinnable polylactide (PLA) matrix.[4–6] ZnO is classified in a group of inorganic antimicrobial agents that are safer and extremely thermally stable compared to organic antimicrobial agents.[7] It is already used in personal care products and in prosthetic devices for hard-tissue replacement.[8] We studied the antibacterial properties of ZnO when it was finely dispersed in a polymer. This method guarantees the durability of the antibacterial treatment of the polymer.[9]

Other studies have already been carried out on polymers containing ZnO nanoparticles. In these cases, stable systems have been developed with the retention of their physical properties associated with their size and a chemical activity related to their availability in the matrix.[1] In previous studies, ZnO was incorporated in poly(methyl methacrylate),[10,11] polystyrene,[12] polyamide,[13] polyacrylonitrile,[14] and polyurethane,[15] and the results have shown that the nanocomposites presented better performances compared to the virgin polymers.

In this studied, we examined the incorporation of ZnO nanoparticles into PLA, a synthetic polymer derived from renewable resources. PLA is one of the most interesting biopolymers compared to others such as poly(3-hydroxybutyrate), poly(ε-caprolactone), or poly(glycolic) acid because of its better mechanical and thermal properties and also because of its ease of processing.[16]

Nanocomposites produced from PLA with appropriate amounts of ZnO were used to prepare nanostructured filaments by melt spinning, an ecofriendly solvent free process. Another route, named the *masterbatch (MB) method*, was also investigated to produce nanocomposite multifilaments. The principle of the MB approach was to process filaments with specific amounts of nanofillers directly with the melt-spinning pilot with a highly loaded premix. We studied the influence of this method on the

thermal and mechanical properties of the filaments. Finally, some nanostructured filaments were used to produce knitted fabrics for antibacterial activity assessment.

The antibacterial mechanism of ZnO was also investigated, with the latter not clearly being understood yet.[2] Several mechanisms have been proposed in the literature:

1. Action of reactive oxygen species (ROS).[17–21]
2. Action of zinc ions.[22,23]
3. Mechanical damage of cells.[23]

Yamamoto[6] and Sawai *et al.*[24] reported that the mechanical destruction of the cell membrane had no effect on the antibacterial activity of the ceramic powder. Therefore, we concentrated our efforts on studying the contribution of zinc ions or/and ROS on the antibacterial activities of ZnO through different analytical techniques.

EXPERIMENTAL

Materials

Poly(L,L-lactide) grade for fibers [$M_{n(PLA)} = 44{,}900$ g/mol and $M_w/M_n = 1.9$, where $M_{n(PLA)}$ is the number-average molecular weight of PLA, M_w is the weight-average molecular weight and M_n is the number-average molecular weight; D isomer $\approx$ 2%] was kindly supplied by NatureWorks LLC.

Commercially available ZnO nanofillers were graciously donated by Umicore Zinc Chemicals (Belgium) as Zano 20 [particle size $\approx$ 30 nm, bulk density $\approx$ 280 g/L, specific surface area [Brunauer-Emmett-Teller (BET)] = 25–35 m^2/g, ZnO content $\approx$ 99.5%] and as Zano 20 Plus [surface-coated with a triethoxycaprylylsilane especially suitable for the treatment of metal oxides, particle size $\approx$ 30 nm, bulk density $\approx$ 360 g/L, specific surface area (BET) = 25–35 m^2/g, ZnO content $\approx$ 96.2%]. The surface-treated Zano 20 Plus and untreated Zano 20 were named ZnO_T and ZnO_{NT}, respectively. The spin finish, Crosanol I-PA07, was supplied by Eurodye CTC and used for the spinning process on multifilaments. Throughout this contribution, all of the percentages are given as weight percentages.

Processing

Before all processing, the PLA and nanofillers were dried at 80°C for 12 h to minimize the water content during melt compounding. Dried pellets of PLA and appropriate contents of nanofillers (ZnO) were mixed in a turbomixer (1000 rpm, 2 min); this was followed by the dosing and melt compounding into a conventional corotating twin-screw extruder (Lietritz type ZSE 18 HP-40D, screw diameter = 18 mm, length/diameter = 40). The temperatures of the eight heating zones were 190/195/200/200/200/200/200/195°C for PLAs containing 1 and 3% ZnO_T and 180/190/200/195/195/195/190/190°C for the same polymer containing 1 and 3% ZnO_{NT}. The rotation speed of the screws was maintained at 100 rpm for all of the experiments. After melt blending, the nanocomposite extrudate was pelletized and then dried under the previous conditions before spinning.

The PLA and nanocomposites were spin-drawn with a melt-spinning pilot (Spinboy I, designed by Busschaert Engineering). The pellets were melted in a single-screw extruder with temperature profiles of 195/205/210/200/185°C for PLA and PLA/ZnO_T and 175/180/185/175/165°C for PLA/ZnO_{NT}. The molten matrix was then brought through two parallel spinning dies (40 channels with diameters of 400 μm each) heated at 175 and 165°C for PLA, PLA/ZnO_T, and PLA/ZnO_{NT}, respectively, to obtain a continuous multifilament yarn. After extrusion, the yarn was coated with the spin finish Crosanol I-PA07 to ensure its cohesion and to dissipate the static electricity generated during processing. At last, the yarn was hot-drawn between two series of rolls with different rotation speeds. The *draw ratio*, defined as the ratio between the rotation speeds of the drawing and the feeding rolls (150 m/min), was optimized at 3. The temperature of the feeding rolls was fixed at 70°C, whereas the temperature of the drawing roll was fixed at 110°C[25] and 90°C for PLA, PLA/ZnO_T, and PLA/ZnO_{NT}, respectively.

For nanocomposite filaments produced with MB (PLA/30% ZnO_T), the melt-spinning conditions are similar to those of PLA/ZnO_T described previously.

Multifilament yarns made with PLA and some nanocomposites were knitted manually on a rectilinear machine of gauge 7. The as-produced fabrics were used for antibacterial activity testing after the spin finish was removed.

Characterization

X-ray Diffraction (XRD) Analysis. The structural characterization of two types of ZnO (ZnO_{NT} and ZnO_T) was carried out by XRD with a D8 Bruker advance (ZXS) diffractometer (with Cu Kα = 0.15406-nm radiation). The diffraction patterns were produced for values of 2θ between 10 and 80°, with a scan rate of 0.02° and interval measurements of 2 s.

Size Exclusion Chromatography. The recovery of PLA from selected compositions for the molecular weight parameter determination was carried out by the initial dissolution of the samples in chloroform and through a similar procedure used in the case of the PLA/organically modified layered silicate (OMLS) nanocomposites.[26] The metallic residues were removed by liquid–liquid extraction with 0.1*N* HCl aqueous solution; this was followed by intensive washing with demineralized water. Finally, PLA was recovered by precipitation in an excess of heptane. After filtration and drying, the PLA solutions were prepared in THF (10 mg of polymer/5 mL of solvent). The M_n values of the pristine PLA and PLA extracted from the nanocomposites were determined by size exclusion chromatography with a procedure and relations described elsewhere.[26]

Another grade of PLA [$M_{n(PLA')} = 55{,}000$ g/mol, where $M_{n(PLA')}$ is the number-average molecular weight of PLA′] was used for this characterization.

Thermogravimetric Analysis (TGA). TGA was performed with a TGA 2050 instrument (TA Instruments) with a heating ramp of 10°C/min under nitrogen flow from room temperature up to 650°C. Granules (ca. 10 mg) or filaments (ca. 5 mg) were placed in open platinum pans. The precision of the temperature measurements was ±0.5°C.

Electron Probe Microanalysis. A Cameca SX 100 apparatus was used. This device used a voltage of 15 kV, an amperage of 40 nA, and Kα of Zn was detected with a lithium fluoride (LiF)

Table I. Antibacterial Performance Based on *A* Values

A	Antibacterial performance
<0.5	None
0.5 to <1	Slight
1 to <2	Medium
2 to <3	Good
≥3	Very good

crystal. On the color scale (on the right of the image shown later in Figure 3), the red color corresponded to a high concentration of Zn element and so to ZnO concentration.

Mechanical Testing Measurements. Before tensile testing, the average diameters of the filaments (50 measurements per sample) were obtained with an optical microscope (Axiolab Pol, Carl Zeiss). From the diameter and density of PLA, it was then possible to calculate the fineness (tex, g/km). Tensile tests of the PLA and nanocomposite fibers were carried out according to the standard NF EN ISO 5079 on a Zwick 1456 testing machine, with the cell force used being 10 N. All of the tests were made in a standard atmosphere (temperature = 20 ± 2°C and relative humidity = 65 ± 5%). The length between the clamps was fixed at 20 mm, and the speed rate of the crosshead was 20 mm/min. All of the results represent an average value of 30 tests.

Antibacterial Properties. The standard JIS L 1902:2002 was used to conduct antibacterial testing. It is an industrial standard for antibacterial activity assessment on antibacterial textiles. Here, all of the samples (knitted fabrics) were cleaned for 15 min in each solvent (petroleum ether, ethanol, and water) thanks to an ultrasonic tank and were washed according to the NF EN ISO 6330 standard to remove the spin finish. They were then sterilized by steam for 20 min before bacterial inoculation. The samples were seeded with *Staphylococcus aureus* (Gram-positive bacteria) or *Klebsiella pneumonia* (Gram-negative bacteria) bacteria; two strains of bacteria are often responsible of nosocomial infection.[27] This quantitative test method involved the direct counting of bacteria before and after incubation at 37°C for 18 h. The obtained values were used to calculate the antibacterial activity (*A*) according to eq. (1):

$$A = \log C_{18} - \log T_{18} \quad (1)$$

where *C* and *T* are the numbers of bacteria counted from the control (unfunctionalized) and treated (functionalized) textiles and the subscript 18 corresponds to the time of incubation, that is, 18 h. The antibacterial performance was assigned according Table I.

Detection of Zinc Ions (Zn^{2+}). In the presence of moisture or water, ZnO can release Zn^{2+}. The antibacterial action of ZnO is often associated with these ions.[22,28] Specific tests allow the detection and quantification of zinc ions present in aqueous solution when in contact with nanocomposites. The tested solutions were prepared to approximate the conditions of antibacterial testing. An amount of 2 g of fibers (unfunctionalized or functionalized) were immersed in 100 mL of demineralized water, and the whole was stored for about 18 h at 37°C.

Qualitative test. Previous prepared solutions were used to detect the presence of Zn^{2+}. A specific color indicator, Eriochrome Black T (EBT), was used. In fact, at pH 9.5, EBT gives a blue color to the aqueous solution in the absence of Zn^{2+} and a pink color otherwise.

Quantitative test. Inductively coupled plasma (ICP) mass spectrometry (MS) was used for quantitative measurements. A Quadrupole ICP-MS instruments (7500i Agilent) equipped with Ni cones, a glass Scott chamber, and a Babington nebulizer was used. The radio frequency (RF) generator was operated at 1300 W.

Detection of ZnO Defects (Oxygen Vacancies). ZnO is an oxide able to form various defects in connection with the heat treatment it undergoes. One of these defects concerns oxygen vacancies. These vacancies can capture an electron and promote paramagnetic defects. EPR has proven to be a valuable tool for characterizing these kinds of defects.

The spectrometer used was a Bruker EPR ELEXYS E580 operating at the X band of the EPR (9.8 GHz). The microwave power was set to 5 mW, and the amplitude modulation to 1 G. All of EPR spectra were relative to a mass of about 1 mg of nanofillers or nanocomposite filaments.

Detection of ROS [Hydroxyl Radicals (OH˙)] by Spin-Trapping Measurements Coupled with EPR Spectroscopy. EPR coupled with the spin-trapping technique was used to demonstrate the formation of HO˙ radicals in water suspensions of nanocomposite filaments. Fresh distilled 5,5-dimethyl-1-pyrroline-*N*-oxide (DMPO; 0.06*M*) was used as spin trap agent. The concentration added to nanocomposites was 8 m*M* in pure-grade water. The suspension was stirred for a few seconds. The aqueous suspension was then removed and inserted in a narrow quartz tube. The tube was then placed in the EPR cavity, and the spectra were recorded.

For irradiated samples, filaments were irradiated through EPR cavity with polychromatic light (Lightning Cure LC8, Hamamatsu, 100 W) for 20 min before the addition of aqueous solution and DMPO.

RESULTS AND DISCUSSION

The mechanism of the antibacterial activity of ZnO was investigated when it was embedded in a polymeric matrix (PLA). The antibacterial mechanism of ZnO is still discussed in the literature. Some researchers[19,22,24,29–31] think this property is due to the presence of Zn^{2+} and/or ROS (OH˙) when ZnO is in contact of water. We studied the relation between the antibacterial activity of the nanocomposites and the presence of these reactive species in view of evaluating their contribution to the antibacterial mechanism of the nanocomposites.

Some problems, such as a high loss of mechanical and thermal properties, due to the intensive degradation of the polymer matrix[32] occurred with the addition of ZnO to the matrix. One solution for decreasing the action of ZnO on the PLA matrix during melt blending is to use ZnO with a specific surface treatment (e.g., a silane, especially triethoxycaprylylsilane).[32]

Another solution found to decrease once again the negative action of ZnO on the PLA matrix molecular weight is to work

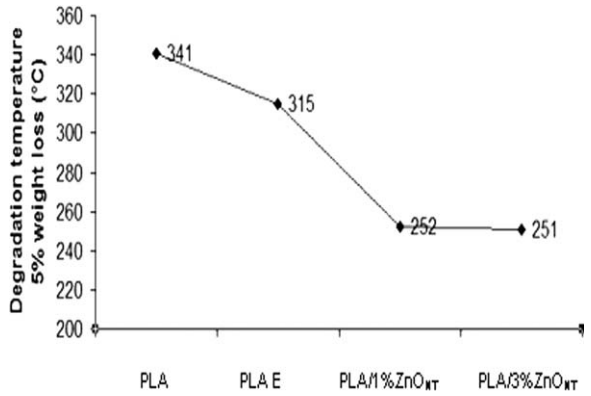

Figure 1. Reduction of the PLA degradation temperature with the extrusion process and the addition of ZnO_{NT}.

with the MB process during the production of nanocomposite filaments. This technique has already been used successfully to improve the properties of other polymer blends.[33,34] Its influence on the thermal and mechanical properties of the nanocomposite filaments was then investigated.

Studies of the PLA Degradation by the ZnO_{NT} Granular Nanocomposites

Figure 1 shows the values of the degradation temperature for 5% weight loss. This temperature is often considered to be the initial decomposition temperature.[35] From the TGA results in Figure 1, we observed an initial decrease in the PLA thermal degradation temperature after the extrusion process of this polymer (where the sample was referred to as PLA E). This result could be explained by the sensitivity of PLA to various phenomena (temperature, shear, and hydrolysis) during processing in the molten state.[35,36] A slight depolymerization of the polymer was then observed after the extrusion process (see Table II). We also noticed a significant decrease in the degradation temperature with the addition of ZnO_{NT} (see Figure 1) and a depolymerization of PLA (see Table II) in the presence of ZnO_{NT}. These results were supported by an article from Abe *et al.*,[37] who reported that under isothermal conditions, zinc compounds catalyze both intermolecular and transesterification reactions and generate PLA with lower molecular weights.

Improvement of the Thermal Degradation Temperature with ZnO_T Granular Nanocomposites

Figure 2 compares the thermal degradation temperatures of the PLA nanocomposites with 1 and 3% ZnO_{NT} and ZnO_T. For 1% nanofillers, the temperature increased about 36°C with ZnO_T

Table II. Reduction of the PLA Molecular Weights with the Extrusion and Addition of ZnO_{NT}

	$M_{n(PLA')}$ (g/mol)
PLA′	55,000
PLA′E	49,900
PLA′/1% ZnO_{NT}	45,600
PLA′/3% ZnO_{NT}	31,300

PLA′ = grade of PLA (M_n = 55000 g/mol); PLA′E = extruded PLA′.

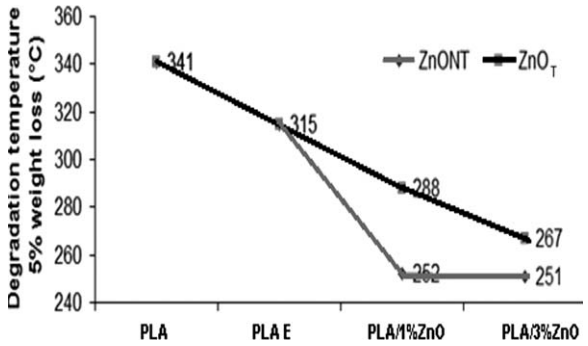

Figure 2. Improvement of the nanocomposite thermal degradation temperatures with ZnO_T.

instead of ZnO_{NT}. For 3%, there was also a temperature increase with ZnO_T but less than previously (ca. 16°C). These results were expected because Das *et al.*[38] reported that a uniform dispersion of highly compatible filler led to a good interaction with the polymer matrix and to improvements in the mechanical and thermal properties of the resulting composite. We found ZnO_T was better dispersed in the PLA matrix (Figures 3 and 4) than ZnO_{NT}. Therefore, this could explain the higher thermal degradation temperatures of the composites including ZnO_T. Also, the siloxane network (triethoxycaprylylsilane) close to the inorganic surface of ZnO_T decreased the catalytic action of ZnO on PLA through a decrease in the PLA depolymerization.[32] Then, the thermal stability of the nanocomposites increased. The previous nanocomposite granules with ZnO_{NT} and ZnO_T were used to produce nanocomposite filaments. In addition to that, the MB process with a high-loaded premix was explored for filament manufacturing.

Studies of the Thermomechanical Properties and Morphology of the Nanocomposite Filaments

A draw ratio of 3 was considered for PLA, extruded PLA, and nanocomposites filaments. Table III shows the degradation temperature (at a 5% weight loss) of PLA, PLA E, and nanocomposites granules and fibers. Figures 5 and 6 show the weight loss versus the temperature.

Nanocomposite granules underwent a second heat and mechanical treatment during the melt-spinning process to produce fibers. This explained why the thermal degradation temperatures of the fibers (Table III, column 3) were lower than those of the granules (Table III, column 2).

Filaments made with nanocomposites containing ZnO_T had degradation temperatures higher than those obtained with ZnO_{NT} (PLA/3% ZnO_{NT}: 244°C and PLA/3% ZnO_T: 251°C). This was due to the lower degradation and depolymerization of PLA by ZnO_T (see Table II).

The last column in Table II (column 4) concerns the nanocomposite filaments obtained from MB. A significant increase in the mentioned temperatures for these filaments could be highlighted. The results obtained in this case were comparable to those of the granules made with ZnO_T. This reflected the low degradation of PLA by this method and could be explained by several factors:

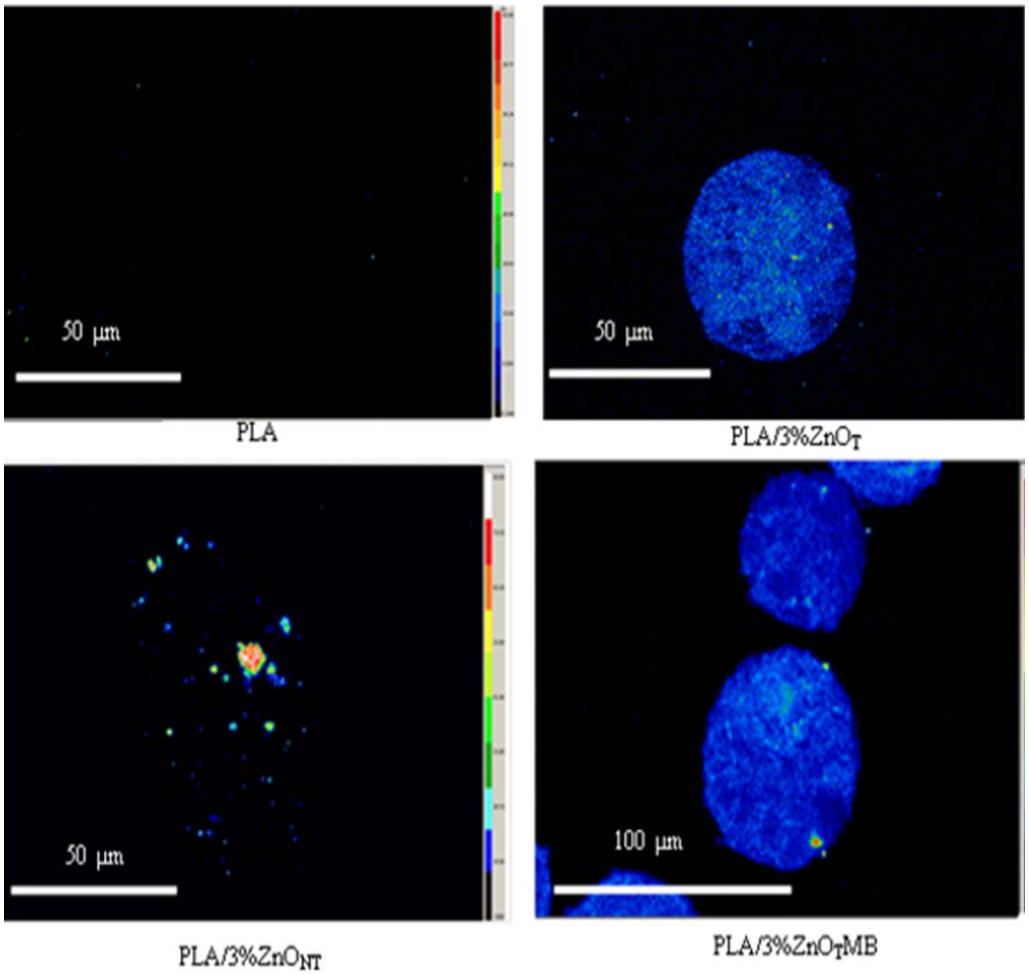

Figure 3. Electron probe microanalysis pictures: filaments (PLA, PLA/3% ZnO_T, PLA/3% ZnO_{NT}, and PLA/3% ZnO_T MB). [Color figure can be viewed in the online issue, which is available at wileyonlinelibrary.com.]

1. A large proportion of the PLA underwent only one thermal cycle during melt-spinning.
2. This proportion was extruded with a single screw, which was less aggressive than twin screws.
3. The nanofillers were first coated with a certain amount of PLA (during MB production) before their dispersion in a large proportion of PLA during the melt-spinning stage to obtain the desired amount of nanofillers in nanocomposite filaments. Thus, precoating decreased the direct contact between ZnO and the large proportion of PLA and also improved the affinity between the nanofillers and PLA.[39]

To compare properly different nanocomposites, the mechanical test results are presented in terms of the percentage change in the tenacity (resistance/linear density). This percentage (given in Figure 7) expresses the reduction in the tenacity compared to virgin PLA filaments.

The best tenacity was obtained with PLA/1% ZnO_T MB. This was due to the low quantity of ZnO_T (1%) and the MB process used; this resulted in the mitigation of PLA degradation (see Table III). Figure 7 also shows the decrease of the tenacity with the augmentation of the nanofiller content. The most fragile filaments were obtained with PLA/3% ZnO_{NT}. This confirmed the degradation of PLA by ZnO_{NT} (see Table III). The poor dispersion of ZnO_{NT} in PLA (see Figure 3) and the formation of aggregates (represented by red dots in the Figure 3 online) could also explain this decrease in the tenacity. With ZnO_T, the silane treatment (layers of —Si—O—Si—O—) led to a lower interfacial energy between the polymer matrix and nanofillers and to the finest dispersion of the nanoparticles in the matrix (see Figures 3 and 4). Das *et al.*[38] reported that the uniform dispersion of highly compatible filler led to good interaction with the polymer matrix and to improvements in the mechanical and thermal properties of the resulting composite.

Antibacterial Properties of the Knitted Fabrics

Knitted fabrics were manufactured from the filaments for antibacterial characterization. It was interesting that despite the degradation of PLA by ZnO, the mechanical properties of the yarns were sufficient to produce knitted fabrics.

Both Gram-positive and Gram-negative bacteria were tested. The results for different nanocomposites are given in Figure 8. All of the values are given as a logarithm (to base 10) and were counted by colony-forming units for each sample. The reported

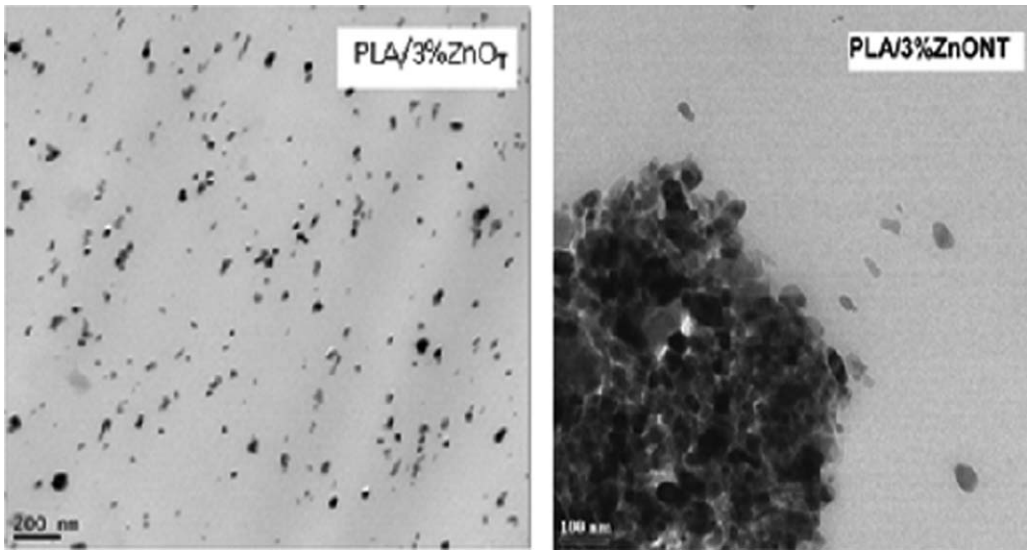

Figure 4. Transmission electron microscopy pictures of the filaments (PLA/3% ZnO_T and PLA/3% ZnO_{NT}).

results are the average values of three samples (see the Experimental section on Antibacterial Properties).

Figure 8 shows that the incorporation of 1% zinc oxide (here ZnO_T) was not sufficient to provide antibacterial properties to the nanocomposites against both tested bacteria. At 3%, the action of ZnO increased, and we noticed a difference in the antibacterial activity depending on the type of bacteria strain and nanofillers (ZnO_T and ZnO_{NT}).

The results obtained (see Figure 8) show that the antibacterial activity of the nanocomposites with ZnO (ZnO_T and ZnO_{NT}) was better on the Gram-positive strain. This result was in agreement with the studies of Sawai *et al.*[40] and Zhang *et al.*[41] In fact, Gram-negative bacteria have lipopolysaccharides in their cytoplasmic membrane that protects them against certain chemical species.[2]

When tested on the Gram-positive bacteria, there was no significant difference between the values of the antibacterial activities of the knitted fabrics realized with PLA/3% ZnO_T (3.3) or PLA/3% ZnO_{NT} (3.2). However, with Gram-negative bacteria, there was a marked increase in the antibacterial activities for PLA/3% ZnO_T (2.9) compared to PLA/3% ZnO_{NT} (1.2). Indeed, because the Gram-negative bacteria were less sensitive to ZnO, the differences in the antibacterial activity between samples were more noticeable and helped us to detect the most efficient type of nanofillers to impart antibacterial activities to PLA.

Table III. Degradation Temperatures at 5% Weight Loss (Granules and Filaments of PLA, PLA E, and Nanocomposites)

	Degradation temperature at 5% weight loss (°C)		
	Granules	Filaments	Filaments (MB)
PLA	341	321	—
PLA E	315	310	—
PLA/1% ZnO_{NT}	252	—	—
PLA/1% ZnO_T	288	258	283
PLA/3% ZnO_{NT}	251	244	—
PLA/3% ZnO_T	267	251	276

Study of the Mechanism of the Antibacterial Properties of the PLA/ZnO Nanocomposites

Crystal Structure and Crystal Defects (Oxygen Vacancies) of Both ZnOs. It is well known that the photocatalytic properties of ZnO are essentially linked to its crystallographic structure and its defects.[42]

A crystallographic difference between the two types of ZnO could explain any difference in the photocatalytic behavior. Figure 9 presents the XRD curves of both ZnO. It showed that two types of ZnO had a würtzite crystal structure. In fact, the distribution of the intensity peaks was consistent with the standard for hexagonal crystals of ZnO,[43,44] and there were no impurities in the crystalline phases.

As mentioned by Tang *et al.*,[45] surface treatment does not affect the ZnO crystal structure. A difference in the crystalline

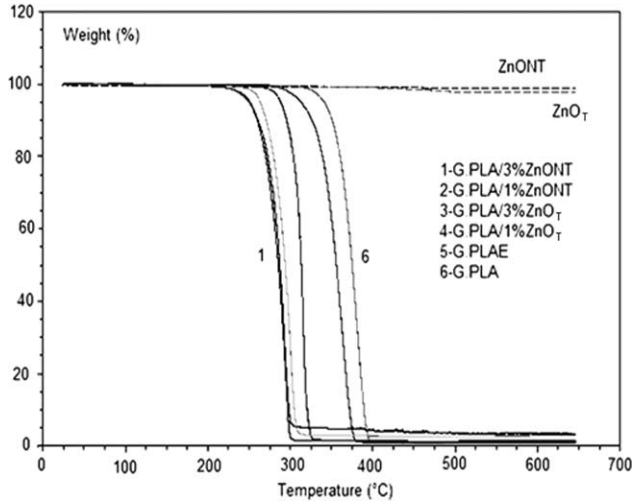

Figure 5. TGA curves of the nanocomposite granules (G) after the extrusion process.

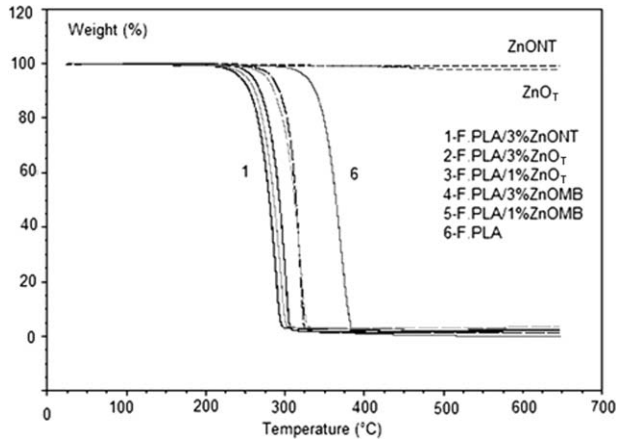

Figure 6. TGA curves of the nanocomposite filaments (F) versus the virgin PLA filaments.

structure could, therefore, not explain any photocatalytic behavior between both ZnOs in this study.

Figure 10 shows the EPR spectra of the nanofillers and qualitatively compares the oxygen vacancies present in the two nanofillers. The spectra consisted of a 9 G line centered at the landé *g* factor value of 1.96 typical of oxygen vacancies defects. The quantity of vacancies was, in fact, related to the area under the peaks of the EPR spectrum. However, we only refer to the intensities of the peaks because their widths were identical. The higher the peak intensities were, the higher was the quantity of oxygen vacancies in the nanofillers; this was important. Figure 10 shows a greater quantity of oxygen vacancies in the case of ZnO_T. Contrary to Guo *et al.*[46] suggested that the intrinsic defects of ZnO nanoparticles could be passivated by capping agents; instead, this study showed that the surface treatment (triethoxycaprylylsilane) performed on ZnO_T increased the amount of oxygen vacancies (and also its defects). On the basis of this result, we established that the surface treatment (triethoxycaprylylsilane) performed on ZnO_T increased the number of oxygen vacancies.

Detection of the HO˙ Radicals. It is well known that ZnO presents photocatalytic properties under the action of UV rays.[47] Fujishima *et al.*[48] reported that these properties existed even under normal lighting (light intensity = 10 mW/cm^2), which contains a certain quantity of UV rays (intensity = 1 mW/cm^2). This quantity was sufficient to cause ZnO photocatalysis, and this led to the formation of ROS, which are harmful to bacterial cells.

Sawai *et al.*[21,24] suggested that hydrogen peroxide (H_2O_2) was responsible for the ZnO antibacterial activity. Zhang *et al.*[41] even suggested that it would be the dominant mechanism. However, Gedanken and coworkers[19,20] identified the formation of HO˙ radicals in an aqueous suspension of ZnO and attributed to them the antibacterial activity of ZnO. HO˙ radicals have indeed a strong oxidizing power,[49] approximately 1.58 times greater than that of H_2O_2.[50] HO˙ is, therefore, more bactericidal than H_2O_2. Reactions leading to the formation of HO˙ are given below:[21,51]

$$e^- + O_2 \longrightarrow O^{\circ}{}_2^-$$

$$O^{\circ}{}_2^- + H_2O \rightleftharpoons HO^{\circ}{}_2 + HO^-$$

$$2HO^{\circ}{}_2 \longrightarrow H_2O_2 + O_2$$

$$e^- + H_2O_2 \longrightarrow HO^{\circ} + HO^-$$

Free electrons generated during ZnO photocatalysis react with oxygen to form superoxide ions. In the presence of moisture, these form hydroperoxyl radicals. Then, the disproportionation of the previous radicals gives H_2O_2. Finally, H_2O_2 reacts with another free electron to form HO˙ radicals. HO˙ radicals are very reactive with bacteria[52] and destroy them by the peroxidation of lipids contained in the cell membrane.[53]

The presence of HO˙ radicals in aqueous suspensions of nanocomposite filaments (especially, PLA/3% ZnO_T and PLA/3% ZnO_{NT}) were checked and qualitatively compared to better understand the difference in the antibacterial effectiveness between these two nanocomposites.

To detect the presence of OH˙, which had a very short lifetime, a spin-trap DMPO was added to the aqueous suspension to form a more stable radical species [DMPO–OH˙]. The latter could be detected by EPR spectroscopy and could be recognized by four characteristic peaks because of hyperfine coupling with the nitrogen and proton of DMPO. The hyperfine constant value *A* related to the electron/nuclei due to electron delocalization on proton and nitrogen atom coupling were respectively $A_H = A_N = 14.5$ G.[54] The quantity of radicals formed was

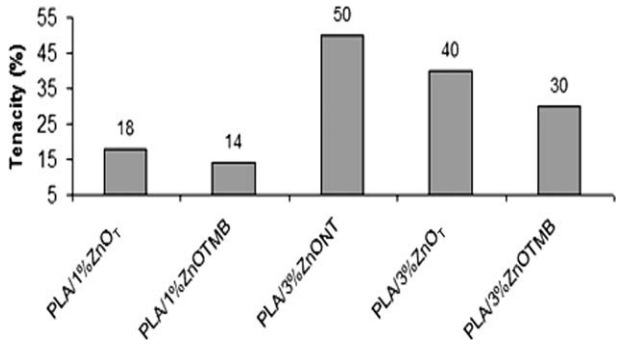

Figure 7. Percentage tenacity reduction of the nanocomposite filaments versus the virgin PLA filaments.

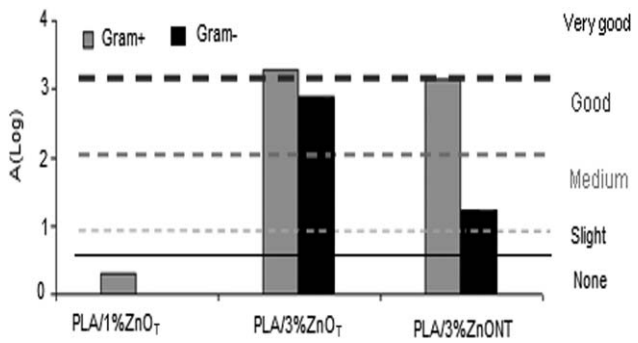

Figure 8. Antibacterial activities results: assessment of the nanocomposite antibacterial activity for both bacterial strains.

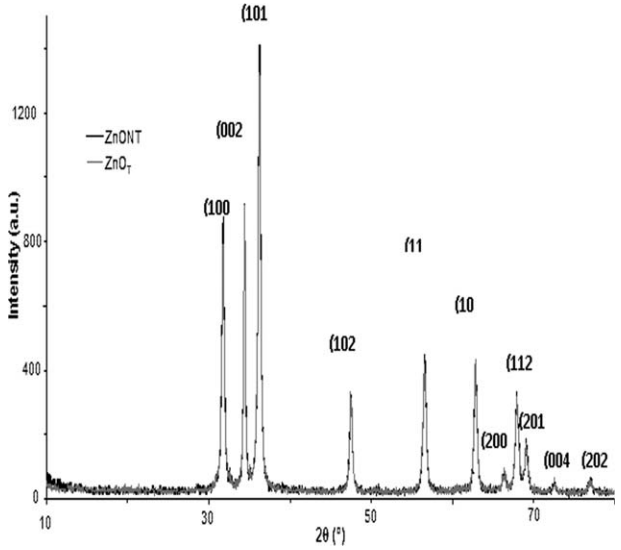

Figure 9. XRD patterns of ZnO on both nanofillers (ZnO_{NT} and ZnO_T).

proportional to the area under the peaks. The higher the intensities were, the higher the quantity of HO˙ radicals was. Figure 11 shows that the intensity of the RPE spectrum of PLA/3% ZnO_T was slightly higher than that of PLA/3% ZnO_{NT}. This means that there were more HO˙ radicals formed in the aqueous solution that was in contact with PLA/3% ZnO_T. This explained the higher antibacterial performance of the fabrics with PLA/3% ZnO_T filaments.

The release of the HO˙ radicals was compared for the nanocomposites irradiated by a polychromatic light (for 20 min). We observed an exceptional increase in the release of OH˙ radicals in the case of PLA/3% ZnO_T (see Figure 12). This study showed the effectiveness of the nanocomposite system with ZnO_T for bacterial decontamination.

The best antibacterial activity obtained with PLA/3% ZnO_T could be explained by the increase in oxygen vacancies; this resulted from the surface treatment of ZnO (see Figure 10) and the good dispersion of ZnO_T in PLA (see Figure 3). Kubacka *et al.*[55] and Heine *et al.*[56] already reported that a good dispersion of nanofillers in the matrix led to better antibacterial activity in the nanocomposite systems. In our case, this statement

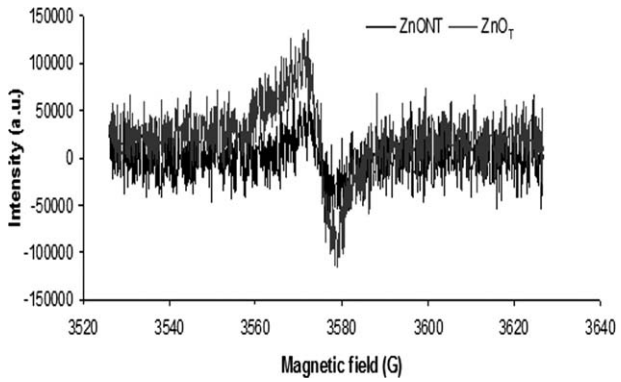

Figure 10. EPR spectra of the nanofillers: detection of oxygen vacancies on both ZnO.

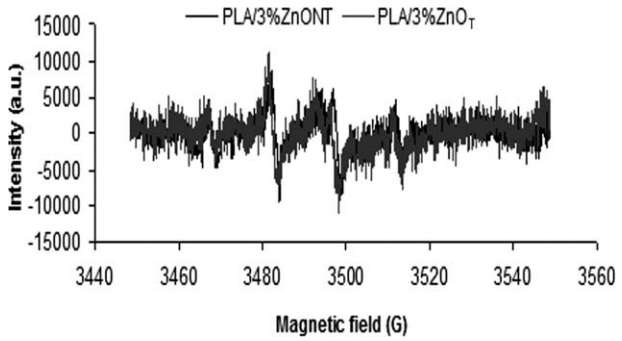

Figure 11. EPR spectra of solutions in contact with the nanocomposites: detection of OH˙.

could be explained by the fact that when the nanofillers were well dispersed, small aggregates with important specific surface areas were formed. It is well known that when nanoparticles have important specific surface areas, they have more active sites on their surface, and therefore, the rate of reaction on its surface increases.[6,57]

Detection of Zn^{2+}. Brunner *et al.*[22] attributed the antibacterial activity of ZnO to dissolved ions (Zn^{2+}). Their presence (qualitatively and quantitatively) was checked in aqueous solutions that had been in contact with filaments (virgin and nanocomposites), and the correlation with the antibacterial activity was verified.

In the qualitative analysis, a color indicator (EBT) was placed in the solutions. A blue color was observed for the solution with virgin PLA filaments, and a pink color was observed for solutions with nanocomposite filaments (see Figure 13). This means that

1. There are no Zn^{2+} ions in the reference solution (solution with virgin PLA filaments). This was normal and allowed us to validate the qualitative test method.
2. There were Zn^{2+} ions in the other solutions that were in contact with the nanocomposites.

We used ICP to quantitatively detect the amount of Zn^{2+} in the aqueous solutions that were in contact with the nanocomposites.

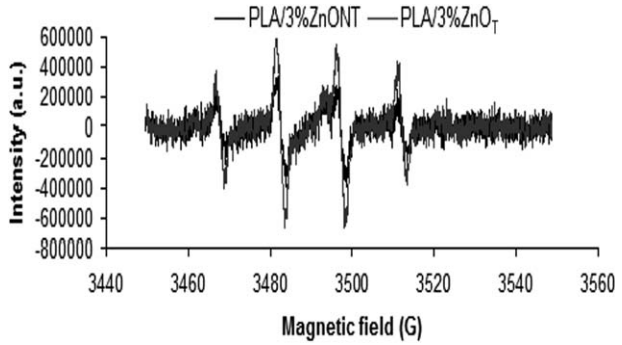

Figure 12. EPR spectra of solutions in contact with the irradiated nanocomposites: detection of OH˙.

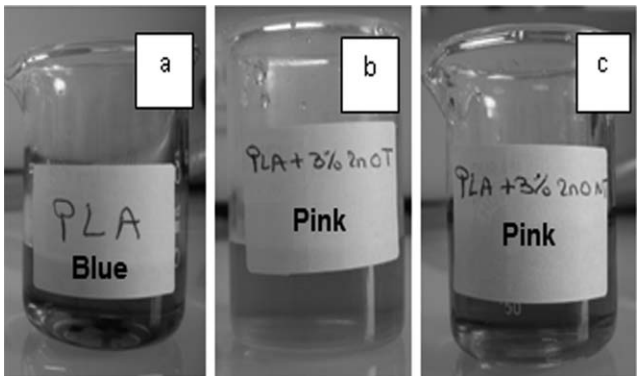

Figure 13. Images of different solutions in the presence of EBT.

Table IV presents the results for ICP analysis. Rigorously, ICP analysis quantifies the quantity of zinc element (Zn) rather than Zn^{2+} ions. However, taking into account the qualitative results, we equated Zn with Zn^{2+}.

As expected, there were no traces of Zn^{2+} ions in the aqueous solution containing PLA fibers.

The two solutions gave positive qualitative results and contained Zn^{2+} ions. The solution with PLA/3% ZnO_{NT} filaments contained 1813 µg/L Zn^{2+}, and the other with PLA/3% ZnO_T contained 497 µg/L Zn^{2+}. The low formation of Zn^{2+} ions in the second case could be explained by the hydrophobic surface treatment (with silane) on ZnO_T. This decreased the effect of the aqueous solution on ZnO and led to fewer Zn^{2+} ions formed.

We have, however, already shown that the antibacterial activity was better with PLA/3% ZnO_T (see Figure 8). Because of this result, the antibacterial performance of the samples could not be related to the presence of Zn^{2+}. The solution with PLA/3% ZnO_T contained, in fact, less Zn^{2+}.

Moreover, the quantity of ions measured in solutions with both nanocomposites was very low. These low concentrations were probably far from the minimum inhibitory concentration for antibacterial activity of Zn^{2+}. Indeed, Applerot *et al.*[19] reported that a concentration of 25 mg/L Zn^{2+} had no effect on certain bacteria, including *S. aureus* bacteria. These bacteria were used during antibacterial testing in this study (see Figure 8) and were more sensitive to the action of ZnO than the other bacteria, *K. pneumonia*. We, hence, deduced that the antibacterial properties of the studied nanocomposites were not due to Zn^{2+} ions. Dutta and coworkers[58,59] already reported the negligible release of zinc ions from ZnO nanoparticles (NPs) in aqueous medium and also concluded that the inhibition of bacterial growth due to released zinc ions was ruled out.

Table IV. Concentrations of Zn^{2+} in Different Solutions

	Zn^{2+} (µg/L)
PLA	0
PLA/3% ZnO_T	497
PLA/3% ZnO_{NT}	1813

CONCLUSIONS

An antibacterial and inorganic nanoadditive (ZnO) was used to functionalize PLA by an extrusion process. The obtained granules were used to process multifilament yarns before the characterization of their antibacterial properties (knitted structure).

We showed the initial degradation of the PLA matrix by ZnO_{NT}. However, the addition of ZnO_T led to a decrease in this degradation. Then, the better thermal and mechanical properties were achieved on nanocomposites containing ZnO_T. In fact, ZnO_T was better dispersed in PLA and had a lower impact on its degradation through depolymerization.[32]

The MB process was used to produce multifilaments to better protect PLA against the action of ZnO during melt-spinning process. This resulted in an increase in the degradation temperature and the tenacity of these filaments.

We found better antibacterial properties with the nanocomposite containing 3% nanofillers (instead of 1% nanofillers). Also, better antibacterial activity was achieved with PLA/3% ZnO_T thanks to the good dispersion of ZnO_T into PLA. This higher dispersion promoted nanocomposite photocatalysis and led to the formation of an important quantity of HO˙ radicals, which had a strong bactericidal action. Also, we found that at a measured concentration of Zn^{2+} ions, they had some impact on the antibacterial activity of the studied nanocomposites.

ACKNOWLEDGMENTS

The authors thank the Wallonia Region, the Nord-Pas de Calais Region, and the European Community for its financial support in the framework of the INTER-REGIONAL Fourth call for projects program-NANOparticules pour la production de materiaux performants et biodegradables a base d'acide polyLACtique (INTERREG IV-NANOLAC) project. They thank all partners, especially Philippe Dubois (Materia Nova, Mons, Belgium) and his collaborators and Serge Bourbigot (Ecole Nationale Supérieure de Chimie de Lille, Lille, France) and his collaborators, for helpful discussions. They also thank all of the companies mentioned for supplying the raw materials and Institut Pluridisciplinaire Hubert CURIEN (IPHC) for ICP-MS analyses.

REFERENCES

1. Balta, S.; Sotto, A.; Luis, P.; Benea, L.; Van der Bruggen, B.; Kim, J. *J. Membr. Sci.* **2012**, *389*, 155.
2. Amornpitoksuk, P.; Suwanboon, S.; Sangkanu, S.; Sukhoom, A.; Muensit, N. *Superlattices Microstruct.* **2012**, *51*, 103.
3. Sun, J. H.; Dong, S. Y.; Wang, Y. K.; Sun, S. P. *J. Hazard. Mater.* **2009**, *172*, 1520.
4. Tam, K. H.; Djurisic, A. B.; Chan, C. M. N.; Xi, Y. Y.; Tse, C. W.; Leung, Y. H.; Chan, W. K.; Leung, F. C. C.; Au, D. W. T. *Thin Solid Films* **2008**, *516*, 6167.
5. Hu, W.; Shiyan, C.; Zhou, B.; Wang, H. *Mater. Sci.* **2005**, *249*, 76.
6. Yamamoto, G. *Int. J. Inorg. Mater.* **2001**, *3*, 643.
7. Jalai, R.; Goharshad, E. K.; Abareshi, M.; Moosavi, M.; Yousefi, A.; Nancarrow, P. *Mater. Chem. Phys.* **2010**, *121*, 345.

8. Saha, N.; Keskinbora, K.; Suvaci, E.; Basu, B. *J. Biomed. Mater. Res. Part B* **2010**, *95*, 430.
9. Bonin, L. E. Ph.D. Thesis, University of Louisiana at Lafayette, **2008**.
10. Sun, D.; Miyatake, N.; Sue, H. *J. Nanotechnol.* **2007**, *18*, 215606.
11. Demir, M. M.; Memesa, M.; Castignolles, P.; Wegner, G. *Macromol. Rapid Commun.* **2006**, *27*, 763.
12. Ma, C.; Chen, Y. J.; Kuan, H. C. *J. Appl. Polym. Sci.* **2005**, *98*, 2266.
13. Wu, M.; Yang, G. Z.; Wang, M.; Wang, M. Z.; Zhang, W. D.; Feng, J. C.; Liu, T. X. *Mater. Chem. Phys.* **2008**, *109*, 547.
14. Chae, D. W.; Kim, D. C. *J. Appl. Polym. Sci.* **2006**, *99*, 1854.
15. Ma, X. Y.; Zhang, W. D. *Polym. Degrad. Stab.* **2009**, *94*, 1103.
16. Uruyama, H.; Kanamori, T.; Kimura, Y. *Macromol. Mater. Eng.* **2002**, *287*, 116.
17. Dutta, R. K.; Nenavathu, B. P.; Gangishetty, M. K.; Reddy, A. V. *Colloids Surf. B* **2012**, *94*, 143.
18. Raghupathi, K. R.; Koodali, R. T.; Manna, A. C. *Langmuir* **2011**, *27*, 4020.
19. Applerot, G.; Lipovsky, A.; Dror, R.; Perkas, N.; Nitzan, Y.; Lubart, R.; Gedanken, A. *Adv. Funct. Mater.* **2009**, *19*, 842.
20. Lipovsky, A.; Tzitrinovich, Z.; Friedmann, H.; Applerot, G.; Gedanken, A.; Lubart, R. *J. Phys. Chem. C* **2009**, *113*, 15997.
21. Sawai, J.; Kawada, E.; Kanou, F.; Igarashi, H.; Hashimoto, A.; Kokugan, T.; Shimizu, M. *J. Chem. Eng. Jpn.* **1996**, *29*, 627.
22. Brunner, T. J.; Wick, P.; Manser, P.; Spohn, P.; Grass, R. N.; Limbach, L. K.; Bruinink, A.; Stark, W. *J. Environ. Sci. Technol.* **2006**, *40*, 4374.
23. Sawai, J.; Kojima, H.; Igarashi, H.; Hashimoto, A.; Shoji, S.; Takehara, A.; Sawaki, T.; Kokugan, T.; Shimizu, M. *J. Chem. Eng. Jpn.* **1997**, *30*, 1034.
24. Sawai, J.; Shoji, S.; Igarashi, H.; Hashimoto, A.; Kokugan, T.; Shimizu, M.; Kojima, H. *J. Ferment. Bioeng.* **1998**, *86*, 521.
25. Solarski, S. Ph.D. Thesis, Université des Sciences et Technologies de Lille 1, **2006**.
26. Paul, M. A.; Alexandre, M.; Degée, P.; Henrist, C.; Rumonlt, A.; Dubois, P. *Polymer* **2003**, *44*, 443.
27. Kerkeni, A. Ph.D. Thesis, Université de Valencienne et de Haut Cambresis, **2010**.
28. Wei, J.; Mashayekhi, H.; Xing, B. *Environ. Pollut.* **2009**, *157*, 1619.
29. Pasquet, J.; Chevalier, Y.; Pelletier, J.; Couvala, E.; Bouvier, D.; Bolzinger, M. A. *Colloids Surf. A* **2014**, *457*, 263.
30. Lipovsky, A.; Nitzan, Y.; Gedanken, A.; Lubart, R. *Nanotechnology* **2011**, *22*, 105101.1.5.
31. Fang, X.; Yu, R.; Li, B.; Somasundaran, P.; Chandran, K. *J. Colloid Interface Sci.* **2010**, *348*, 329.
32. Murariu, M.; Doumbia, A.; Bonnaud, L.; Dechieft, A.-L.; Paint, Y.; Ferreira, M.; Campagne, C.; Devaux, E.; Dubois, P. *Biomacromolecules* **2011**, *12*, 1762.
33. Ahmed, S. I.; Shamey, R.; Christie, M.; Mather, R. R. *Color. Technol.* **2006**, *122*, 282.
34. Kim, D. J.; Seo, K. H.; Hong, K. H.; Kim, S. Y. *Polym. Eng. Sci.* **1999**, *39*, 500.
35. Carrasco, F.; Pagès, P.; Gámez-Pérez, J.; Santana, O. O.; Maspoch, M. L. *Polym. Degrad. Stab.* **2010**, *95*, 2508.
36. Hall, E. S.; Kolstad, J. J.; Conn, R. S. E.; Gruber, P. R.; Ryan, C. M. U.S. Pat. 6,335,772 **2002**.
37. Abe, H.; Takahashi, N.; Kim, K. J.; Mochizuki, M.; Doi, Y. *Biomacromolecules* **2004**, *5*, 1606.
38. Das, K.; Ray, D.; Bandyopadhyay, N. R.; Sahoo, S.; Mohanty, A. K.; Misra, M. *Compos. B* **2011**, *42*, 376.
39. Joo, M.; Auras, R.; Almenar, E. *Carbohydr. Polym.* **2011**, *86*, 1022.
40. Sawai, J.; Igarashi, H.; Hashimoto, A.; Kokugan, K.; Shimizu, M. *J. Chem. Eng. Jpn.* **1995**, *28*, 288.
41. Zhang, L.; Jiang, Y.; Ding, Y.; Povey, M.; York, D. *J. Nanopart. Res.* **2007**, *9*, 479.
42. Bond, G. C. Heterogeneous Catalysis: Principle and Applications, 2nd ed.; Oxford University Press: New York, **1987**.
43. Maensiri, S.; Laokol, P.; Promarak, V. *J. Cryst. Growth* **2006**, *289*, 102.
44. Yang, Z.; Zong, X.; Ye, Z.; Zhao, B.; Wang, Q.; Wang, P. *Biomaterials* **2010**, *31*, 7534.
45. Tang, E.; Cheng, G.; Ma, X. *Powder Technol.* **2006**, *161*, 209.
46. Guo, L.; Yang, S.; Yang, C.; Yu, P.; Wang, J.; Ge, W.; Wong, G. K. L. *Appl. Phys. Lett.* **2000**, *76*, 2901.
47. Daneshvar, N.; Aber, S.; Seyed Dorraji, M. S.; Khataee, A. R.; Rasoulifard, M. H. *Sep. Purif. Technol.* **2007**, *58*, 91.
48. Fujishima, A.; Rao, T. N.; Tryk, D. A. *J. Photochem. Photobiol. C* **2000**, *1*, 1.
49. Wang, Y.; Huang, F.; Pan, D.; Li, B.; Chen, D.; Lin, W.; Chen, X.; Li, R.; Lin, Z. *Chem. Commun.* **2009**, *44*, 6783.
50. Fujihira, M.; Satoh, Y.; Osa, T. *Bull. Chem. Soc. Jpn.* **1982**, *55*, 666.
51. Mercier, J. P.; Maréchal, E. *Traité Mater. Chim. Polym. Synth. React. Degrad.* **1996**, *13*, 424.
52. Moody, C. S.; Hassa, H. M. *Proc. Natl. Acad. Sci. U. S. A.* **1982**, *79*, 2855.
53. Jiang, W.; Mashayekhi, H.; Xing, B. *Environ. Pollut.* **2009**,*157*, 1619.
54. Buettner, G. R. *Free Radical Biol. Med.* **1987**, *3*, 259.
55. Kubacka, A.; Cerrada, M. L.; Serrano, C.; Fernàndez-Garcia, M.; Ferre, M. *J. Phys. Chem. C* **2009**, *113*, 9182.
56. Heine, E.; Knops, H. G.; Schaefer, K.; Vangeyte, P.; Moeller, M. *Mater. Sci.* **2007**, *97*, 23.
57. Yamamoto, O.; Hotta, M.; Sawai, J.; Sasamoto, T.; Kojima, H. *J. Ceram. Soc. Jpn.* **1998**, *1238*, 1007.
58. Dutta, R. K.; Nenavathu, B. P.; Gangishetty, M. K. *J. Photochem. Photobiol. B* **2013**, *126*, 105.
59. Dutta, R. K.; Nenavathu, B. P.; Gangishetty, M. K.; Reddy, A. V. R. *J. Environ. Sci. Health A* **2013**, *48*, 8871.